

# X-RAY EVOLUTION OF ACTIVE GALACTIC NUCLEI IN HIERARCHICAL GALAXY FORMATION

N. Menci

INAF-Osservatorio Astronomico di Roma, Via di Frascati 33, 00040 Monteporzio (Roma), Italy

## ABSTRACT

We have incorporated the description of the X-ray properties of Active Galactic Nuclei (AGNs) into a semi-analytic model of galaxy formation, adopting physically motivated scaling laws for accretion triggered by galaxy encounters. Our model reproduces the level of the cosmic X-ray background at 30 keV; we predict that the largest contribution (around 2/3) comes from sources with intermediate X-ray luminosity  $10^{43.5} < L_X/\text{erg s}^{-1} < 10^{44.5}$ , with 50 % of the total specific intensity produced at  $z < 2$ . The predicted number density of X-ray AGNs is characterized by a “downsizing” effect: for luminous X-ray AGNs ( $L_X > 10^{44.5}$  erg/s in the 2-10 keV band) it peaks at  $z \approx 2$  with a decline of around 3 dex to  $z = 0$ ; for the low luminosity sources ( $10^{43} < L_X/\text{erg s}^{-1} < 10^{44}$ ) it has a broader and less pronounced maximum around  $z \approx 1.5$ , and a smoother decline at lower  $z$ . We compare our results with recent observations.

Key words: galaxies: active – galaxies: formation – X-rays: galaxies – galaxies: evolution.

## 1. INTRODUCTION

Connecting the evolution of AGNs to that of their host galaxies is a major goal of present “ab initio” galaxy formation models within a cosmological context (see, e.g., Haiman & Loeb 1998; Wyithe & Loeb 2002; Hatziminaoglou et al. 2003; Volonteri, Hardt & Madau 2003; Kauffmann & Haehnelt 2000, 2002). However, a common problem of the models proposed so far is that they do not match the observed steep decline of the QSO density at redshifts  $z \lesssim 1$  and its dependence on the AGN luminosity.

Recently, Menci et al. (2003) developed a physical model to connect the BH accretion to the galaxy evolution in the hierarchical scenario. The accretion is triggered by galaxy encounters, not necessarily leading to bound merging, in common host structures like clusters and especially groups; these events destabilize part of the

galactic cold gas and hence feed the central BH, following the physical modelling developed by Cavaliere & Vittorini (2000). The amount of the cold gas available, the interaction rates, and the properties of the host galaxies are derived through the SAM developed by Menci et al. (2002).

As a result, at high  $z$  the protogalaxies grow rapidly by hierarchical merging; meanwhile, much fresh gas is imported and also destabilized, so the BHs are fueled at their full Eddington rates. At lower  $z$ , the dominant dynamical events are galaxy encounters in hierarchically growing groups; now refueling peters out, as the residual gas is exhausted while the destabilizing encounters dwindle. With no parameter tuning other than needed for star formation in canonical SAMs, the model naturally produces in the bright QSO population a rise for  $z > 3$ , and for  $z \lesssim 2.5$  a drop as steep as observed. In addition, the results closely reproduce the observed luminosity functions of the optically selected QSOs, their space density at different magnitudes from  $z \approx 5$  to  $z \approx 0$ , and also the local  $m_{BH} - \sigma$  relation.

Here we report the implications of this model for the X-ray AGNs (Menci et al. 2004) to derive their contribution to the X-ray background and their intrinsic luminosity function.

## 2. THE GALAXY FORMATION MODEL

The model we adopt is described in detail in Menci et al. (2003; 2004). Here we recall the basic points:

We follow the merging histories of DM clumps, adopting the Extended Press & Schechter description (see, e.g., Lacey & Cole 1993). When two haloes merge, the contained galaxies merge on a longer timescale, either with the central dominant galaxy (due to the orbital decay produced by dynamical friction) or with other “satellite” galaxies orbiting the same DM halo (“binary aggregations”). We describe the potential depth of the DM halo associated to a single galaxy through its circular velocity  $v$ , while the circular velocity of the halos hosting the galaxies (groups and clusters) is  $V$ ; the model also com-

putes the tidal radius  $r_t$  associated to galaxies with given  $v$ .

The properties of the gas and stars contained in the galactic DM clumps are computed following the standard recipes commonly adopted in SAMs. Starting from an initial gas amount  $m \Omega_b / \Omega$  ( $m \propto v^3$  being the DM mass of the galaxies) at the virial temperature of the galactic halos, we compute the mass  $m_c$  of cold baryons which are able to radiatively cool in the densest, central regions. This settles a rotationally supported disk whose radius  $r_d$  and rotation velocity  $v_d$  is computed after Mo, Mao & White (1998). Stars form with rate  $\dot{m}_* \propto (m_c/t_d)$  with the disk dynamical time evaluated as  $t_d = r_d/v_d$ . Finally, a mass  $\Delta m_h = m_* (v/v_h)^{\alpha_h}$  is returned from the cool to the hot gas phase due to the energy fed back by canonical type II Supernovae associated to  $m_*$ . The values adopted for the free parameters  $\alpha_* = -1.5$ ,  $\alpha_h = 2$  and  $v_h = 150$  km/s fit both the local B-band galaxy LF and the Tully-Fisher relation, as illustrated by Menci et al. (2002). The model also matches the bright end of the galaxy B-band LFs up to redshifts  $z \approx 3$  and the resulting global star formation history is broadly consistent with that observed up to redshift  $z \approx 4$  see Menci et al. (2005).

At each merging event, the masses of the different baryonic phases are replenished by those in the merging partner; the further increments  $\Delta m_c$ ,  $\Delta m_*$ ,  $\Delta m_h$  from cooling, star formation and feedback are recomputed on iterating the procedure described above.

The resulting star formation rate (for a given  $v$ ) is convolved with the spectral energy distribution  $\phi_\lambda$  obtained from population synthesis models Bruzual & Charlot (1993) to obtain the integrated galactic stellar emission  $S_\lambda(v, t)$  at the wavelength  $\lambda$ .

### 3. ENCOUNTERS TRIGGERING STARBURSTS AND BH ACCRETION

A quantitative model to derive the fraction  $f$  of cold gas destabilized by the encounters has been worked out by Cavaliere & Vittorini (2000) and has been inserted into a SAM by Menci et al. (2003, 2004, 2005).

For a galactic halo with given circular velocity  $v$  inside a host halo (group or cluster) with circular velocity  $V$  and virial radius  $R$ , grazing encounters occur at a rate  $\tau_r^{-1} = n_T(V) \Sigma(v, V) V_r(V)$ , where  $n_T = 3 N_T / 4\pi R^3$ , and the cross section  $\Sigma(v, V) \approx \pi \langle r_t^2 + r'_t{}^2 \rangle$  is averaged over all partners with tidal radius  $r_t$  and circular velocity  $v'$  in the same halo  $V$ . The membership  $N_T(V)$  (i.e., the number of galaxies contained in a group or cluster with circular velocity  $V$ ), the distributions of  $v'$ ,  $r'_t$ , and the relative velocity  $V_r = \sqrt{2} V$  are computed from the SAM. The duration of each encounter is defined as  $\tau_e = \langle (r_t + r'_t) / V \rangle$  (with an upper limit given by  $\tau_r$ ).

The fraction of cold gas which is destabilized in each in-

teraction event and feeds the starbursts is derived from eq. A3 of Cavaliere & Vittorini (2000) in terms of the variation  $\Delta j$  of the specific angular momentum  $j \approx Gm/v_d$  of the gas;

$$f(v, V) \approx \frac{1}{2} \left| \frac{\Delta j}{j} \right| = \frac{1}{2} \left\langle \frac{m'}{m} \frac{r_d}{b} \frac{v_d}{V} \right\rangle. \quad (1)$$

The average runs over the probability of finding a galaxy with mass  $m'$  in the same halo  $V$  where the galaxy  $m$  is located, and the impact parameter  $b$  is computed in the SAM. The prefactor accounts for the probability 1/2 of inflow rather than outflow related to the sign of  $\Delta j$ .

We assume that 1/4 of the destabilized fraction  $f$  feeds the central BH (whose initial seeds are assumed to have a mass  $10^2 M_\odot$ , see Madau & Rees (2000), while the remaining fraction is assumed to kindle circumnuclear starbursts, see Sanders & Mirabel (1996). Thus, the average gas accretion rate onto the central black hole as

$$\dot{m}_{acc}(v, z) = \left\langle \frac{f(v, V) m_c(v)}{4 \tau_r(v, V)} \right\rangle, \quad (2)$$

where the average over all host halos with circular velocity  $V$  is computed from the SAM. The bolometric luminosity so produced by the QSO hosted in a given galaxy is then given by

$$L(v, t) = \frac{\eta c^2 \Delta m_{acc}}{\tau_e}, \quad (3)$$

where  $\Delta m_{acc}$  is the gas accreted at the rate given by eq. (3). and we adopt the standard mass-to-energy conversion efficiency  $\eta \approx 0.1$  (see Yu & Tremaine 2002). Here  $\tau_e \approx t_d \sim 5 \cdot 10^7 (t/t_0)$  yrs is the duration of the accretion episode, i.e., the timescale for the QSO to shine;  $\Delta m_{acc}$  is the gas accreted at the rate given by eq. (2). The blue luminosity  $L_B$  is obtained by applying a bolometric correction 13 (Elvis et al. 1994), while for the unabsorbed X-ray luminosity  $L_X$  (2-10 keV) we adopt a bolometric correction  $c_{2-10} = 100$  following Elvis, Risaliti & Zamorani (2002); for simplicity, this is assumed to be constant with  $z$ . The shape of the X-ray spectrum  $I(E)$  is assumed to be a power law with a slope  $\alpha = 0.9$  (see Comastri 2000 and references therein), with an exponential cutoff at an energy  $E_c = 300$  keV (see e.g. Perola et al. 2002 and references therein); in view of the present data situation we shall keep this as our fiducial shape.

### 4. RESULTS

We first compute the predicted contribution to the cosmic X-ray background (CXB) from AGNs at different redshifts and luminosity. The result is shown in Fig. 1, for the hard CXB at  $E_0 = 30$  keV obtained by integrating all the predicted sources out to running redshift  $z$ . We show both the global value, and the fraction contributed by AGNs in three classes of luminosity. The predicted background with the chosen parameters for the spectrum

( $\alpha = 0.9$ ,  $E_c = 300$  keV,  $c_{2-10} = 100$ ) exceeds the value measured by HEAO1-A2 by no more than 50 %. Note that the value of the observed background is appreciably affected by the presence of sources in a Compton thick phase of obscuration, not included in the model.

At the present state of our observational knowledge, the substantial agreement is very encouraging, especially if the following points are taken into account: a) the available evidence (at  $E < 10$  keV, Lumb et al. 2002; Vecchi et al. 1999) that the CXB normalization from the HEAO1-A2 experiment may be underestimated by as much as 30 %; b) the bolometric correction need take on the fixed value we adopted for all values of  $L$  and  $L/L_{edd}$ ; c) the incidence of a Compton thick phase along the active phase of a galactic nucleus, as a function of  $L$  and  $z$ , is not known, except that locally it may amount as much as 50 % (Risaliti, Maiolino & Salvati 1999) of the so-called type 2 AGNs, namely those with a substantial obscuration both in the optical as well as in the X-ray band. The essential features of our predictions are shown in Figs. 2 and 3.

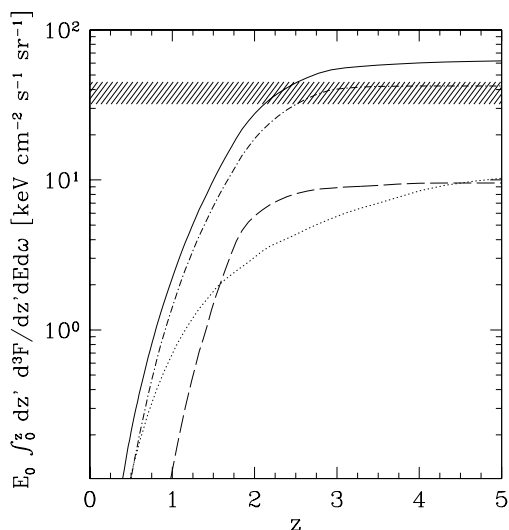


Fig. 2. - The cumulative contribution (multiplied by the energy  $E_0$ ) to the predicted CXB at  $E_0 = 30$  keV, yielded by sources at progressively larger redshifts. The solid line shows the total CXB produced by sources with all luminosities. The other lines show the contributions of AGNs with luminosities  $L_x$  (in units of  $\text{erg s}^{-1}$  in the band 2-10 keV) in the ranges  $42 < \log L_X < 43.5$  (dotted),  $43.5 < \log L_X < 44.5$  (dot dashed), and  $44.5 < \log L_X$  (long-dashed). The shaded strip is the value  $43 \text{ keV cm}^{-2} \text{ s}^{-1} \text{ sr}^{-1}$  measured by HEAO1-A2 (Gruber et al. 1999).

Fig. 1 shows that in our model the CXB is mainly contributed by AGNs with intermediate luminosities  $L_X = 10^{43.5} - 10^{44.5} \text{ erg/s}$ , which provide  $\approx 50\%$  of the total value. High luminosity ( $L_X > 10^{44.5} \text{ erg/s}$ ) and low luminosity ( $L_X < 10^{43} \text{ erg/s}$ ) sources contribute a fraction  $\sim 25\%$  each. The population with intermediate luminosities strikes the best tradeoff between larger luminosity and smaller number of sources. Thus, in this picture high

luminosity highly absorbed objects (the so-called type 2 QSOs) would not give a dominant contribution to the hard CXB. In fact, although recent XMM and Chandra surveys are providing a sizeable number of QSO2 (Barger et al. 2002, Fiore et al. 2003, Hasinger 2003), these are likely to constitute a relatively minor fraction of sources down to the fluxes where the bulk of the hard CXB is resolved into sources.

In Fig. 2 we compare our predictions with the evolution of the number and luminosity densities of AGNs in three luminosity bins, estimated by Fiore et al. (2003). All the predicted densities drop substantially from  $z \approx 2$  to the present. The agreement with the data is excellent for the highest luminosity bin, and confirms that, at least for the very luminous AGNs, the bolometric corrections adopted in the B and in the X-ray band are fully consistent.

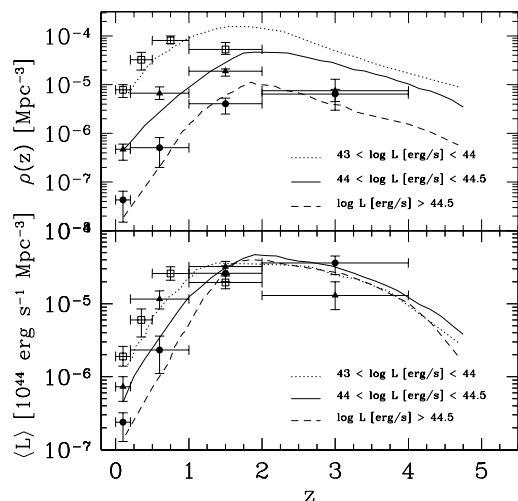


Fig. 2. - Top: The evolution of the number density of X-ray AGNs in three bins of luminosity (in units of  $\text{erg/s}$ , in the band 2-10 keV):  $43 < \log L_X < 44$  (dotted line),  $44 < \log L_X < 44.5$  (solid line),  $44.5 < \log L_X$  (dashed line). The data for the above luminosity bins (squares, triangles, and circles, respectively) are taken from Fiore et al. (2003). Bottom: The evolution of the X-ray luminosity density for the same luminosity bins.

At lower luminosities, the decline for  $z < 1 - 2$  is less pronounced in the predictions as well as in the observations. In the former, this is due to the larger quantity of galactic cold gas left available for accretion in the less massive galaxies. Such a downsizing effect is a natural feature in hierarchical scenarios, since more massive potential wells originate from clumps collapsed earlier in *biased* regions of the primordial perturbation field; the higher densities then prevailing allowed for earlier condensation and hence enhanced star formation at high redshifts. Thus, at low  $z$  a larger fraction of cold gas will have already been converted into stars, and both star formation and BH accretion are considerably suppressed. We note though that the decrease of the peak redshift with decreasing luminosity appears to be significantly smaller than indicated by the data. In particular, at  $z = 1 - 2$  the observed density of Seyfert-like AGNs is a factor  $\approx 2$

lower than predicted by the model; a similar difference is present also for the intermediate luminosity objects ( $L_{2-10} = 10^{44-44.5} \text{ erg s}^{-1}$ ) in the redshift bin  $z = 2-4$ .

The reason for such a discrepancy can be traced back to the shape of the high- $z$  X-ray luminosity function. This is shown in Fig. 3, where we compare our model results with the observational LFs derived by Fiore et al. (2003, upper panel) and by Ueda et al. (2003, lower panel), which are obtained from a combination of HEAO1, ASCA and *Chandra* data, and extend down to lower luminosities. The above observational results concur to indicate that the LFs at  $z \gtrsim 2$  are appreciably flatter than at  $z = 0.5 - 1$ . When the above data are compared to our results, a substantial agreement is found at low  $z$ , while at  $z \gtrsim 1.5 - 2$  the model overestimates the number of low luminosity objects found in both the observational analysis. Such a mismatch can not be reduced by tuning the bolometric correction  $c_{2-10}$  adopted in our model, since the latter affects only the normalization of the luminosities.

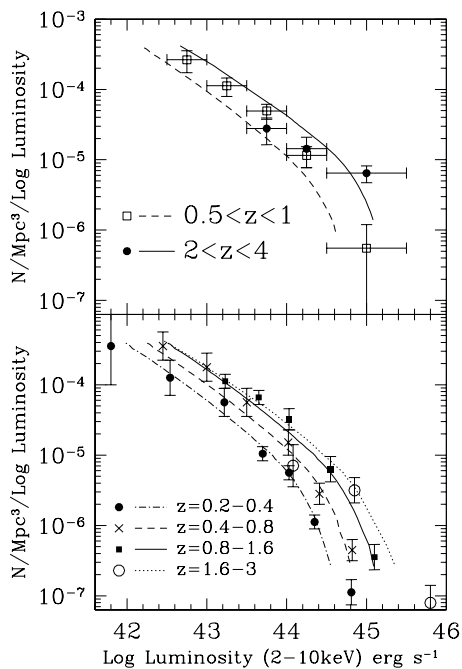


Fig. 3. - Upper panel. The predicted LFs in the energy range 2-10 keV at low redshifts  $0.5 < z < 1$  (dashed line) and high redshifts  $2 < z < 4$  (solid line) are compared with observational values derived from the same sample used in Fiore et al. (2003) to derive the densities in Fig. 2. Bottom panel. The predicted LFs are compared with data by Ueda et al. (2003).

## 5. DISCUSSION

We have incorporated the description of the X-ray properties of AGNs into the hierarchical picture of galaxy evolution. Our semi-analytic model, already proven to

match the observed evolution of luminous optically selected QSOs over the redshift range  $0 < z < 6$  (Menci et al. 2003), is here extended to bolometric luminosities  $L$  a factor 10 lower. So we describe the history of accretion down to  $L \sim 10^{45} \text{ erg/s}$ , for which the main observational information comes from the X-ray band.

We have compared our model with X-ray observations either corrected for gas obscuration, or performed in the hard ( $E > 30 \text{ keV}$ ) band not affected by photoelectric absorption.

We find that our model is encouragingly able to match the level of the cosmic X-ray background (CXB) at 30 keV (Fig. 1). We predict that the largest contribution (around 2/3) to the CXB comes from intermediate luminosity sources  $43.5 < \log(L_X/\text{erg s}^{-1}) < 44.5$ , and that 50 % of its total specific intensity is produced at  $z < 2$ .

When compared to the observed evolution of the number and luminosity density of AGNs with different  $L_X$  (Fig. 2), our model agrees with the observations concerning all luminosities  $L_X > 10^{43} \text{ erg/s}$  for low or intermediate redshifts  $z \lesssim 1.5 - 2$ . In particular, the density of luminous ( $L_X > 10^{44.5} \text{ erg/s}$ ) AGNs peaks at  $z \approx 2$ , while for the low luminosity sources ( $10^{43} < L_X/\text{erg s}^{-1} < 10^{44}$ ) it has a broader maximum around  $z \approx 1.5$ ; the decline from the maximum to the value at the present epoch is around 3 dex for the former class, and 1.5 dex for the latter class. At larger redshifts  $z \gtrsim 2$ , the model still reproduces the observed number and luminosity densities of AGNs stronger than  $10^{44.5} \text{ erg/s}$ , but at  $z = 1 - 2$  the predicted density of Seyfert-like AGNs is a factor  $\approx 2$  larger than observed; a similar difference is present also for the intermediate luminosity objects ( $L_{2-10} = 10^{44-44.5} \text{ erg s}^{-1}$ ) in the redshift bin  $z = 2 - 4$ . We next discuss our interpretation of both the low- $z$  and the high- $z$  results.

For  $z \lesssim 2$ , the model results agree with the observed number and luminosity densities in indicating a drop of the AGN population for  $z < 2$  which is faster for the strongest sources. Such a *downsizing* effect in our picture is due to the combined effect of: 1) the decrease of the galaxy merging and encounter rates which trigger the gas destabilization and the BH feeding in each galaxy; 2) of the decrease of the galactic cold gas, which was already converted into stars or accreted onto the BH. The faster decline which obtains in massive galaxies (and hence for luminous AGNs) is related in particular to the latter effect. Indeed, in hierarchical clustering scenarios the star formation history of larger objects peaks at higher  $z$ , since massive objects originate from progenitors collapsed in biased regions of the Universe where/when the higher densities allowed for earlier star formation; so, at low  $z$  such objects have already exhausted most of their gas. On the other hand, less massive galaxies are continuously enriched by low-mass satellites, whose star formation is more smoothly distributed in  $z$ , and which retain even at  $z \approx 0$  an appreciable fraction of cold gas available for BH accretion.

Although the model naturally yields a downsizing effect, we note though that the decrease of the peak redshift with decreasing luminosity appears to be smaller than indicated by the data. Such mismatch is even larger if the model predictions for the AGN number density are compared with the recent data by Hasinger, Miyaji & Schmidt (2005; see also this volume). However, it must be considered that our model does not include absorption: thus, the comparison with the absorption-corrected data by Fiore et al. (2003) in the harder 2-10 keV band constitutes a more solid baseline for probing the model predictions.

A real improvement in the modeling requires the inclusion of additional physical processes in the SAM (and in particular in the sector concerning the feedback) rather than the tuning of the parameters in the existing framework. One such process could be well constituted by the inclusion into SAMs of the feedback produced by the AGNs emission itself. Since the AGN activity strongly increases with redshift, this could significantly contribute to expell/reheat part of the galactic cold gas reservoir in low-mass systems at high  $z$ . While the modeling of such impulsive processes is particularly delicate, some steps in this direction have already been taken (see, e.g., Haehnelt, Natarajan & Rees 1998; Silk & Rees 1998; Wyithe & Loeb 2003; Cavaliere, Lapi & Menci 2002; and references therein). We shall investigate the effects of such processes on the evolution of the AGN population in a next paper.

In sum, the present model provides a baseline to include the evolution of galaxies and AGNs in the same global picture, being supported by a remarkable agreement with the observations of its predictions for brighter sources in a wide range of redshifts (from  $0 < z < 6$ ) and of wavelengths (from optical to X-rays). The most distinctive feature of such a picture is the dramatic decrease of the AGNs luminosities at  $z \lesssim 2$  especially in massive galaxies (see Fig. 1), naturally resulting from the exhaustion of cold gas necessary for feeding both the accretion and the star formation; relatedly, massive galaxies are predicted to undergo a nearly passive evolution from  $z \approx 2$  to the present. The relevance of such an exhaustion in determining the observed properties of the AGN population (in both the optical and the X-rays) is confirmed by recent N-body simulations (Di Matteo et al. 2003). The above picture thus naturally explains the parallel evolution of BH accretion and star formation in spheroidal systems; this, originally discussed by Monaco, Salucci & Danese (2000) and Granato et al. (2001), is supported by recent works (see Franceschini, Hasinger, Miyaji, Malquori 1999; Haiman, Ciotti & Ostriker 2003) which also enlightened its simultaneous consistence with the evolution of the optical and the X-ray luminosity functions of AGNs (Cattaneo & Bernardi 2003). The physical origin of such a parallel evolution is here clarified and shown to arise as a natural outcome of hierarchical galaxy formation.

## REFERENCES

- Barger, A., Cowie L., Brandt, W.N., Capak, P., Garnire, G.P., Hornschemeier, A.E., Steffen, A.T., & Wehner, E.H. 2002, *AJ*, 124, 1839
- Bruzual, A.G., & Charlot, S., 1993, *ApJ*, 105, 538
- Cattaneo, A., & Bernardi, M. 2003, *MNRAS*, 344, 45
- Cavaliere, A., Vittorini, V., 2000, *ApJ*, 543, 599
- Cavaliere, A., Lapi, A., & Menci, N. 2002, *ApJ*, 518, L1
- Comastri, A. 2000, in *Stellar Endpoints, AGN, and the Diffuse X-ray Background*, Ed. N. White, G. Malaguti, G.G.C. Palumbo, AIP conference proceedings, 599, 73
- Comastri, A., Fiore, F., Vignali, C., Matt, G., Perola, G.C., La Franca, F., 2001, *MNRAS*, 327, 781
- Di Matteo, T., Croft, R.A.C., Springel, V., Hernquist, L. 2003, *ApJ*, 593, 56
- Fiore, F. et al. 2003, *A&A*, 409, 79
- Franceschini, A., Hasinger, G., Miyaji, T., Malquori, D., 1999, *MNRAS*, 310, L5
- Granato, G.L., Silva, L., Monaco, P., Panuzzo, P., Salucci, P. De Zotti, G., Dbibitem, 2001, *MNRAS*, 324, 757
- Gruber, D.E. et al., 1999, *ApJ*, 520, 124
- Haehnelt, M., & Rees, M.J., 1993, *MNRAS*, 263, 168
- Haehnelt, M., Natarajan, P., & Rees, M.J., 1998, *MNRAS*, 300, 817
- Haiman, Z., Loeb, A. 1998, *ApJ*, 503, 505
- Haiman, Z., Ciotti, L., Ostriker, J.P., 2003, preprint [astro-ph/0304129]
- Hasinger, G. 2003, proceedings of the Conference: The Emergence of Cosmic Structure, Maryland, Stephen S. Holt and Chris Reynolds (eds), astro-ph/0302574
- Hatziminaoglou, E., Mathez, G., Solanes, J.-M., Manrique, A., Salvador-Sole, E., 2003, *MNRAS*, 343, 692
- Kauffmann, G., Haehnelt, M., 2000, *MNRAS*, 311, 576
- Kauffmann, G., Haehnelt, M., 2002, *MNRAS*, 332, 529
- Lacey, C., & Cole, S., 1993, *MNRAS*, 262, 627
- Lumb, D.H., Warwick, R.S., Page, M., De Luca, A., 2002, *A&A*, 389, 93
- Madau, P., & Rees, M.J., 2000, *ApJ*, 551, L27
- Menci, N., Cavaliere, A., Fontana, A., Giallongo, E., Poli, F., 2002, *ApJ*, 578, 18
- Menci, N., Cavaliere, A., Fontana, A., Giallongo, E., Poli, F., Vittorini, V. 2003, *ApJ*, 587, L63

- Menci, N., Fiore, F., Perola, G.C., Cavaliere, A., 2004, *ApJ*, 606, 58
- Menci, N., Fontana, A., Giallongo, E., Salimbeni, S. 2005, *ApJ*, 632, 49
- Mo, H.J., Mao, S., & White, S.D.M., 1998, *MNRAS*, 295, 319
- Monaco, P., Salucci, P., Danese, L. 2000, *MNRAS*, 317, 488
- Perola, G.C., Matt, G., Cappi, M., Fiore, F., Guainazzi, M., Maraschi, L., Petrucci, P.O., Piro, L. 2002, *A&A*, 389, 802
- Poli, F. et al. 2003, *ApJ*, 593, L1
- Risaliti, G. Maiolino, R. & Salvati, M. 1999, *ApJ*, 522, 157
- Sanders, D.B., & Mirabel, I.F. 1996, *ARA&A*, 34, 749
- Silk, J., & Rees, M.J. 1998, *A&A*, 331, 1
- Ueda, Y., Akiyama, M., Ohta, K., Miyaji, T., 2003, preprint [astro-ph/0308140]
- Vecchi, A., Molendi, S., Guainazzi, M., et al. 1999, *A&A*, 349, L73
- Volonteri, M., Haardt, F., Madau, P., 2003, *ApJ*, 582, 559
- Yu, Q., & Tremaine, S., 2002, *MNRAS*, 335, 965
- Wyithe, J.S., Loeb, A. 2002, *ApJ*, 581, 886
- Wyithe, J.S., Loeb, A. 2003, *ApJ*, 595, 614